Appl Microbiol Biotechnol (2007) 77:175–182
DOI 10.1007/s00253-007-1125-3

ENVIRONMENTAL BIOTECHNOLOGY

Effects of aeration intensity on formation of phenol-fed aerobic granules and extracellular polymeric substances

Sunil S. Adav · Duu-Jong Lee · J. Y. Lai

Received: 1 June 2007 / Revised: 11 July 2007 / Accepted: 13 July 2007 / Published online: 21 August 2007

Abstract Effect of air aeration intensities on granule formation and extracellular polymeric substances content in three identical sequential batch reactors were investigated. The excitation–emission–matrix spectra and multiple staining and confocal laser scanning microscope revealed proteins, polysaccharides, lipids, and humic substances in the sludge and granule samples. Seed sludge flocs were compacted at low aeration rate, with produced extracellular polymeric substances of 50.2–76.7 mg g^{-1} of proteins, 50.2–77.3 mg g^{-1} carbohydrates and 74 mg g^{-1} humic substances. High aeration rate accelerated formation of 1.0–1.5 mm granules with smooth outer surface. The corresponding quantities of extracellular polymeric substances were 309–537 mg g^{-1} of proteins, 61–109 mg g^{-1} carbohydrates, 49–92 mg g^{-1} humic substances, and 49–68 mg g^{-1} lipids. Intermediate aeration rate produced 3.0–3.5 mm granules with surface filaments. Reactor failure occurred with overgrowth of filaments, probably owing to the deficiency of nutrient in liquid phase. No correlation was noted between extracellular polymeric substances composition and the proliferation of filamentous microorganisms on granule surface.

S. S. Adav · D.-J. Lee (✉)
Department of Chemical Engineering,
National Taiwan University,
Taipei 10617, Taiwan
e-mail: djlee@ntu.edu.tw

J. Y. Lai
Department of Chemical Engineering, R&D Center of Membrane Technology, Chung Yuan Christian University,
Chungli 32023, Taiwan

Keywords Aeration · EPS · Granule formation · Filaments

Introduction

The aerobic granule process has been extensively investigated (Morgenroth et al. 1997; Beun et al. 1999; Tay et al. 2001; Liu and Tay 2004). Most studies have focused on granule cultivation via various substrates or on treatment efficiency of various granule processes (Arrojo et al. 2004; Kim et al. 2004; McSwain et al. 2004; Wang et al. 2004; Hu et al. 2005). High hydrodynamic shear is known to produce compact, dense, and strong granules (Liu and Tay 2002; Tay et al. 2004).

Extracellular polymeric substances (EPS) are crucial in building and maintaining structural integrity of aerobic granules through cohesion and adhesion of microbial cells (Morgan et al. 1990; Lopes et al. 2000; Wu et al. 2006; Hwang et al. 2006). Quarmby and Forster (1995) reported a weakened granular structure in EPS-deficient aerobic granules. After heating at 80°C in the presence of NaOH or using cation exchange resins to extract EPS from granules, Tay et al. (2001) and Wang et al. (2005) concluded that increased hydrodynamic shear increases polysaccharide production in granules. However, McSwain et al. (2005) concluded that proteins, rather than polysaccharides, enrich granules.

This study investigated the effect of air aeration on granule formation and incorporated EPS content. The EPS were extracted by six different schemes and compared. The chemical nature and spatial location of the granules were examined by excitation-emission matrix (EEM) spectra and multiple staining-confocal laser scanning microscopy (CLSM; Chen et al. 2007). Possible causes of filament overgrowth on granules were then examined.

Materials and methods

Reactor operation and samples

Aerobic-activated sludge was collected from a local municipal wastewater treatment plant in Taipei, Taiwan. The sludge sample was inoculated in three geometrically identical acrylic columns of 80-cm height, and 6-cm in diameter was and aerated with 1.0–3.0 l min^{-1} air from the reactors' base. The columns were fed with synthetic wastewater containing phenol as a sole carbon source with the following composition: 1,000 mg l^{-1} $(NH_4)_2SO_4$; 200 mg l^{-1} $MgCl_2$; 100 mg l^{-1} NaCl; 20 mg l^{-1} $FeCl_3$; 10 mg l^{-1} $CaCl_2$; phosphate buffer (1,350 mg l^{-1} KH_2PO_4, 1,650 mg l^{-1} K_2HPO_4); pH 6.8 and, micronutrients (g l^{-1}), H_3BO_3, 0.05; $ZnCl_2$, 0.05; $CuCl_2$, 0.03; $MnSO_4.H_2O$ $(NH_4)_6$, 0.05; $Mo_7O_{24}.4H_2O$, 0.05; $AlCl_3$, 0.05; $CoCl_2.6H_2O$, 0.05; and NiCl, 0.05 (Moy et al. 2002). The medium was sterilized via autoclaving for 15 min at 121°C. The phenol solution was filtered and added to the autoclaved medium. The reactor was operated in 12-h cycles. The granules formed and matured in 3 weeks.

Extraction of EPS

The EPS was extracted from sludge or granule samples. Figure 1 illustrates the details of the EPS extraction processes. As a control, the EPS was physically extracted with high speed centrifugation (10,000×*g*) for 20 min without adding chemicals. Some sludge or granule samples were first extracted by NaOH with or without pretreatment using formaldehyde or formamide. The extracts were then filtered and analyzed. In some tests, low frequency ultrasound at 120 W was utilized for 5 min in an ice bath before or after the chemical extraction. Hence, six extraction procedures were tested and compared: formaldehyde + NaOH, ultrasound + formaldehyde + NaOH, formaldehyde + NaOH + ultrasound, formamide + NaOH, ultrasound + formamide + NaOH, and formamide + NaOH + ultrasound. After extraction, all samples were centrifuged and filtered through 0.2 μm filters to collect soluble fractions.

Chemical analysis

The dry weight of granules and volatile suspended solids (VSS) and sludge volume index (SVI) in the samples were measured according to Standard Methods (APHA 1998). The carbohydrate content in EPS was measured by the anthrone method (Gaudy 1962) with glucose as the standard. The protein and humic content in EPS was measured by the modified Lowry method (Frolund et al. 1995) using bovine serum albumin and humic acid (Fluka, USA) as the respective standards. The DNA content was measured by the diphenylamine colorimetric method using fish DNA as the standard. The total lipid content, polar, and neutral lipid, were extracted separately from sludge and granules by the treatment described above and then adding methanol/chloroform (1:2 *v*/*v*). After 5 min centrifugation, the supernatant was treated with sodium chloride (0.9% *w*/*v*). The mixture was centrifuged, and the organic phase (oily phase) was recovered as a lipid extract. Total lipid content was obtained by evaporating the organic solvents and drying in the oven at 45°C for 15 min and accurately weighing.

EEM fluorescence spectroscopy

The EEM spectra of extracted EPS for sludge and aerobic granule samples were recorded by luminescence spectrometry (Cary Eclipse, Varian, USA). The EEM spectra were obtained by scanning the sample for both excitation and emission wavelengths from 200 to 550 nm. The blank EEM spectrum obtained for double distilled water was used to ensure the quality of the scanned samples. For all the measurements, excitation and emission slits were maintained at 5 nm, and 290-nm emission cutoff filter was used to eliminate second order Raleigh light scattering. EEM spectra are illustrated as the elliptical shape of contours where *X*-axis represents the emission spectra from 200 to 550 nm and *Y*-axis as the excitation wavelength from 200 to 550 nm. Forty contour lines, as the third dimension, are shown for each EEM spectra to represent the fluorescence intensity at an interval of 10.

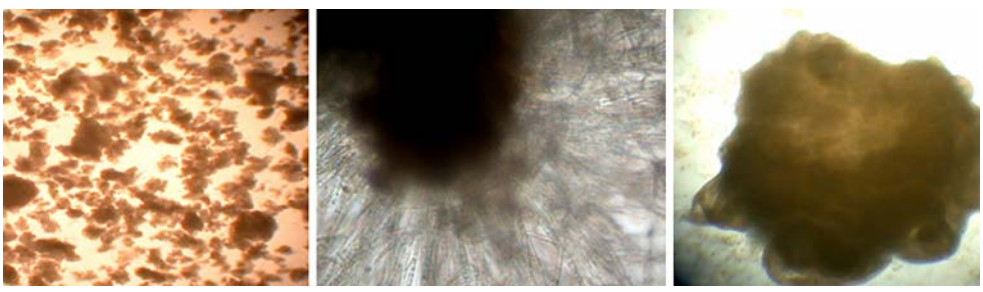

Fig. 1 Microscopic observations of aerobic granules by day 90. **a** R1, **b** R2, and **c** R3

Staining and CLSM imaging

Proteins in the samples were stained with fluoresceinisothiocyanate (FITC). Concanavalin tetramethylrhodamine conjugate (ConA) was used to bind to α-mannopyranosyl and α-glucopyranosyl sugar residues. The whole cells were probed with the wall-permeable nucleic acid stain SYTO 63. The dead cells were stained by cell wall-impermeable stain SYTOX blue. Nile red was used to stain lipids. Calcofluor white was used to stain β-polysaccharides. All probes were purchased from Molecular Probes (Carlsbad, CA, USA).

CLSM (Leica TCS SP2 Confocal Spectral Microscope Imaging System, Germany) was used to visualize cell or EPS distributions in bio-samples. The fluorescence of SYTO 63 was detected via excitation at 633 nm and emission at 650–700 nm. The fluorescent intensity of SYTOX blue was analyzed via excitation at 458 nm and emission at 460–500 nm. The fluorescence of Nile red, FITC, and Calcofluor white were detected via excitation at 514, 448, and 400 nm and emission at 625–700, 500–550, and 410–480 nm, respectively. Staining details are available in Chen et al. (2007).

Results

Granule development

The structure of the sludge flocs in R1 was compacted during incubation but failed to aggregate into large granules (Fig. 1a). Granule formation was observed in reactors R2 and R3 after 3 weeks of incubation (Fig. 1a and b). Importantly, the R3 granules under higher shear were 1.0–1.5 mm and had a smooth outer surface after 160 days of operation. However, those under intermediate shear in R2 were 3.0–3.5 mm and began to exhibit filament growth after day 60 and overgrowth by day 150 (Fig. 1c). The apparent selective pressure of hydrodynamic shear on filament development on granule surface has apparently not been reported previously.

Figure 2a shows chemical oxygen demand (COD) removal rates from reactors R1–R3. The R1 removal rate gradually increased from 75% to approximately 81% by day 80 and thereafter, indicating slow pellet-like accumulation of acclimated microbes in the sludge flocs. The COD removal rate in R2 rapidly increased from 75 to 89% by day 30 upon granule formation. The removal rate then further increased to 95% by day 90 with fully developed surface filaments. Overgrowth of filaments caused granule overflow, thus reducing COD removal rate to 85% on day 160. The corresponding removal rate in R3 increased from 75 to 86% by day 50, stabilized until day 100 then further increased to 97% by day 140.

The SVI values for sludge/granules in R1–R3 all gradually declined (Fig. 2b). The SVI values for pellet flocs in R1 decreased monotonically from 120 to 52 ml g^{-1} by day 160. The R2 and R3 granules yielded SVI lower than 40 ml g^{-1} by day 100. Those in R3 further decreased to 35 ml g^{-1} by days 140–160 while those in R2 recovered to 61 ml g^{-1} by day 160, which was consistent with the granule washout observed in overgrown filaments. Parallel measurement revealed that the average settling velocities of granules by day 90 from reactors R2 and R3 were 12.6±8.2 and 26.6±2.0 m h^{-1}, respectively.

Extracted EPS

Table 1 and Fig. 3 summarize the quantities of EPS extracted from the R1–R3 sludge/granules using the six extraction processes. The quantities of DNA in all collected EPS were less than 0.6 mg g^{-1} VSS, indicating negligible contamination of collected EPS by intracellular substances.

The EPS extracted from sludge pellets in R1 consisted of 50.2–76.7 mg g^{-1} of proteins, 50.2–77.3 mg g^{-1} carbohydrates and 74 mg g^{-1} humic substances. Restated, the quantity of proteins extracted from the R1 sludge pellets

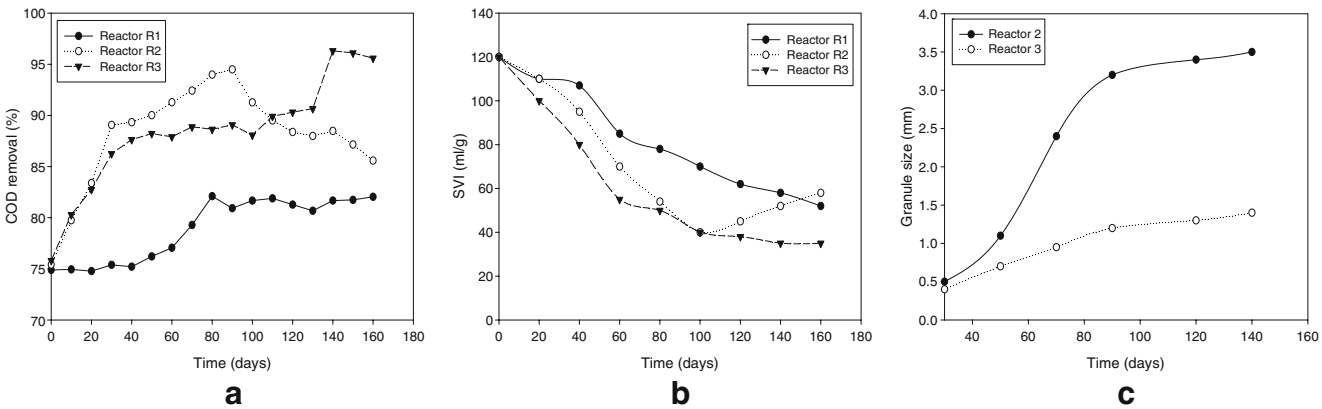

Fig. 2 **a** COD removal rate, **b** SVI, and **c** size of aerobic granular sludge in reactor R1, R2, and R3

Table 1 EPS components of granules cultivated in reactor R1 by various extraction methods

Extraction method	Proteins	Carbohydrates	Humic substances	Lipids	DNA	PN/PS[a]
Formaldehyde–NaOH	66.8±3.3	50.2±7.6	71.6±15.3	15.3±4.3	0.39±0.03	1.41
Formaldehyde–NaOH–ultrasound	66.1±5.0	77.3±27.4	73.3±17.7	19.3±2.5	0.41±0.02	0.86
Ultrasound–formaldehyde–NaOH	76.7±16.8	60.2±24.1	75.9±10.2	21.4±5.2	0.49±0.01	1.28
Formamide–NaOH	50.2±29.3	55.2±23.9	73.5±10.7	14.2±2.9	0.44±0.02	0.91
Formamide–NaOH–ultrasound	64.4±12.1	67.3±21.1	73.4±15.0	15.8±4.9	0.47±0.05	0.96
Ultrasound–formamide–NaOH	69.6±16.2	55.1±15.1	75.9±11.5	17.2±5.2	0.49±0.07	1.26

Unit: mg g^{-1} VSS
[a] *PN/PS* Proteins/polysaccharides ratio

approximated that of polysaccharides (Table 1). Additionally, quantity of extracted EPS was not significantly affected by use of formaldehyde or formamide or by application of ultrasound.

The quantity of proteins extracted from aerobic granules in R1 and R2 exceeded that of extracted polysaccharides (Fig. 3). Formamide extracted a greater quantity of EPS than formaldehyde. Specifically, the extracted EPS in R2 consisted of 256–498 mg g^{-1} of proteins, 55.5–104 mg g^{-1} carbohydrates, 56–93 mg g^{-1} humic substances, and 50–70 mg g^{-1} lipids. The content of R3 was 309–537 mg g^{-1} of proteins, 61–109 mg g^{-1} carbohydrates, 49–92 mg g^{-1} humic substances, and 49–68 mg g^{-1} lipids. Ultrasound reportedly enhances EPS extraction from aerobic granules (Liu and Fang 2002). McSwain et al. (2005) also noted a higher extraction yield in granular samples after homogenization treatment.

EEM characterization of EPS

Three major peaks in the EEM spectra were identified from the collected EPS: excitation/emission wavelengths at peaks A, B, and C were 220–230/340–350 nm, 270–280/340–350 nmm, and Ex/Em 330–340/420–430 nm, respectively. Based on the classification scheme developed by Chen et al. (2003), peaks A, B, and C were in regions II (aromatic proteins), IV (soluble microbial by-product-like), and V (humic acid-like), respectively. The EEM results revealed proteins and humic substances, corresponding to the extraction results for redundant proteins and humic substances.

Table 2 shows the maximum fluorescence peak intensities for peaks A–C. The more proteins and humic substances extracted using the tested scheme (Table 1 and Fig. 3), the stronger the peak intensities in the EEM spectra. Sheng and Yu (2006) proposed that the intensity ratio between peaks B and C (B/C) is useful for chemically analyzing extracted EPS. The (B/C) ratio is generally R1>R2>R3, while the ratio produced by formamide extraction is much higher than that using formaldehyde. Some tests using only ultrasonication without adding chemicals have revealed a (B/C) ratio of 3.0. Hence, the use of formamide in this study may have significantly altered the chemical nature of the extracted EPS.

Characterization of EPS by CLSM

The CLSM images showed low fluorescence for Nile red and calcofluor white in R1 sludge pellets, indicating low lipid and β-polysaccharide content (figure not shown). The quantity of extracted lipids was also low (Table 1).

The R2 granules exhibited extended surface filaments (Fig. 4) with active biomass, protein, and β-polysaccharide accumulating on the outer granular surface. The filaments were hence composed primarily of live cells, proteins,

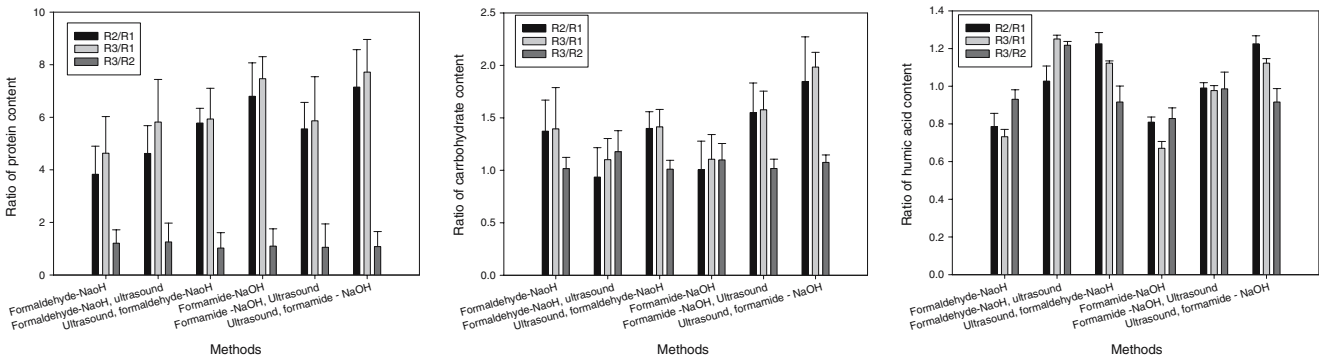

Fig. 3 The ratios of extracted EPS in reactor R1, R2, and R3 using various extraction methods

Table 2 Fluorescence spectral analysis of the EPS extracted by using formaldehyde

Sample	Method	Peak A		Peak B		Peak C		B/C
		Ex/Em	Intensity	Ex/Em	Intensity	Ex/Em	Intensity	
Reactor R1	Formaldehyde–NaOH	220/355	54.9	280/350	132	330/420	42.4	3.12
	Ultrasound–formaldehyde–NaOH	220/350	31.7	270/340	113	330/420	28.8	3.93
	Formaldehyde–NaOH–ultrasound	220/245	33.6	270/345	112	330/430	24.1	4.65
	Formamide–NaOH	220/340	36.7	270/340	795	330/430	14.2	56.0
	Ultrasound–formamide–NaOH	230/320	85.5	270/330	815	330/420	15.8	51.6
	Formamide–NaOH–ultrasound	230/320	118	270/327	935	330/420	19.3	48.6
Reactor R2	Formaldehyde–NaOH	220/360	73.8	270/350	190	330/420	78.6	2.41
	Ultrasound–formaldehyde–NaOH	220/345	60.7	270/350	149	330/420	52.4	2.85
	Formaldehyde–NaOH–ultrasound	220/345	82.3	270/360	186	330/420	53.9	3.45
	Formamide–NaOH	220/340	43.6	270/330	958	330/445	52.5	18.3
	Ultrasound–formamide–NaOH	220/315	114	270/329	982	330/430	43.0	22.9
	Formamide–NaOH–ultrasound	220/320	144	270/275	925	330/440	63.3	14.6
Reactor R3	Formaldehyde–NaOH	220/340	61.4	280/345	173	330/420	78.6	2.19
	Ultrasound–formaldehyde–NaOH	220/350	108	270/355	242	330/420	103	2.36
	Formaldehyde–NaOH–ultrasound	220/350	119	270/355	270	330/420	105	2.58
	Formamide–NaOH	220/340	43.5	270/325	976	330/420	34.4	28.4
	Ultrasound–formamide–NaOH	220/310	108	270/330	917	330/420	39.0	23.5
	Formamide–NaOH–ultrasound	220/230	69.2	270/330	983	330/420	47.6	20.7

lipids, and polysaccharides. This observation correlated with the finding by Adav et al. (2007) that a strain identified as *Candida tropicalis*, which degrades phenol and has a high tolerance to phenol toxicity, could form the filament layers on the granule surface.

The R3 granules exhibited a compact interior structure with a non-cellular core composed mainly of proteins and β-polysaccharides. Living cells on the outer edge of the granule were entrapped with α-polysaccharides and lipids (figure not shown). No extended filaments were noted in R3 granules.

Discussion

Aeration intensity and filaments

In the present study, a low aeration rate (1 l min^{-1}) induced no mature granules but compacted sludge flocs into 300–400 μm pellets. High aeration rate (3 l min^{-1}) yielded mature and stable granules (1–1.5 mm) with compact interior but requiring more aeration. Intermediate aeration (2 l min^{-1}) produced mature and large (3–3.5 mm) granules

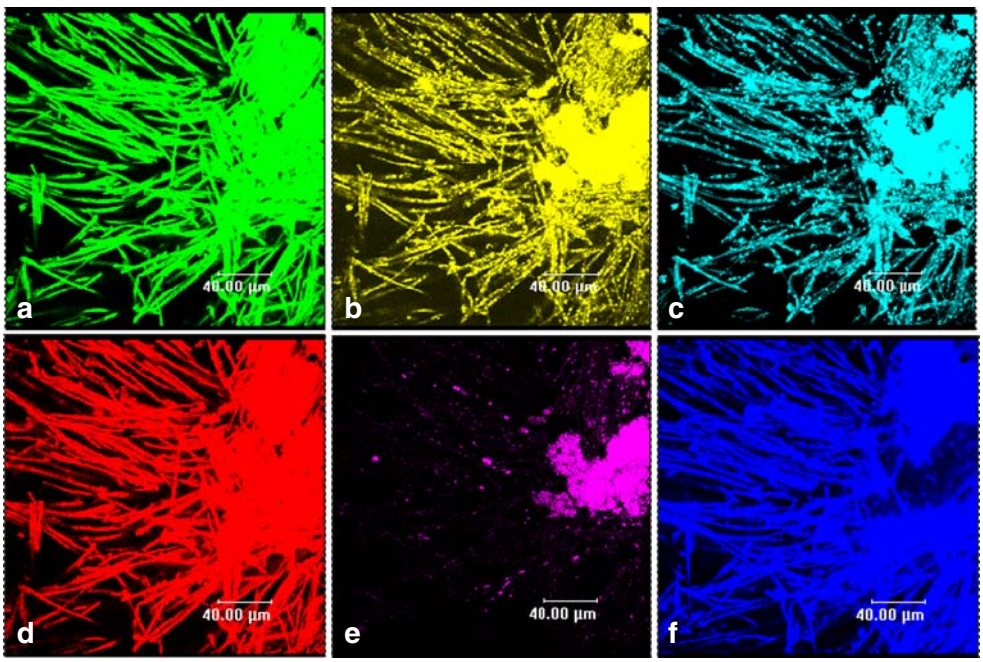

Fig. 4 The CLSM images of granule from reactor R2. **a** *Green (FITC)* Proteins; **b** *yellow (nile red)* lipids; **c** *cyan blue (ConA)* a-D-glucopyranose polysaccharides; **d** *red (SYTO 63)* nucleic acids; **e** *pink (Syto blue)* dead cells, **f** *blue (calcofluor white)* β-D-glucopyranose polysaccharides

but also increased filament overgrowth. Experimental observation revealed that filaments enhanced COD removal in R2 until day 60. However, filament overgrowth yielded granular overflow, and the broken filaments due to aeration shear easily blocked the diffusers and outflow pipelines. Thus, the aeration intensity, treated as an operationally defined parameter herein, manipulated the stability of phenol-fed aerobic granules during column operation.

Deficiencies in dissolved oxygen (DO) or nutrients are favorable for filament growth (Gaval and Pernell 2003; Martins et al. 2003; Rossetti et al. 2005). Liu and Liu (2006) concluded in a review of recent literature that possible causes of filament overgrowth on aerobic granules include (1) long SRT (solid retention time), (2) low substrate concentration in the liquid phase, (3) high substrate gradient within the granule, (4) DO deficiency in the granule, (5) nutrient deficiency within the granule, (6) temperature shift, and (7) disrupted patterns. Items 1, 6, and 7 are operational factors that should not be considered "causes" of filament growth. Conversely, items 2–5 were noted as possible causes because filaments tend to develop over non-filamentous microorganisms when DO and/or nutrient supply is limited. Hence, when mass transfer of the oxygen or substrate is inadequate for replenishing COD degradation within the granule, filaments can only survive by growing outward to compete for available food/DO.

Li et al. (2006) proposed that aged granules tend to accumulate ash solids in their core regimes. Hence, aged granules are more stable than fresh granules in sequencing batch reactor (SBR) operations. However, this theory does not adequately explain the filament-induced system failure noted in the present study.

At aeration rates of 1–3 l min^{-1}, upflow velocities of induced liquid were estimated visually as 5–15 cm s^{-1} at different reactor positions. Hence, the relative velocity of flocs/granules in the aerated columns was of the order of magnitude of 1 cm s^{-1}.

The external mass transfer coefficient around spherical floc or granule of diameter d is given by the following Frossling equation:

$$\mathrm{Sh}\left(\frac{k_c d}{D}\right) = 2.0 + 0.6\,Re^{0.5}\,\mathrm{Sc}^{1/3} \quad (1)$$

where D is the oxygen diffusivity in water (2.2×10^{-9} m^2 s^{-1}), and Sh, Sc, and Re are the Sherwood number, Schmidt number, and Reynolds number, respectively. The Sc for water at 20°C is 435. For flocs in R1 (d=400 mm), as well as granules in R2 (d=1.5 mm) and in R3 (d=3.5 mm), the estimated corresponding k_c values were 5.55×10^{-5}, 2.12×10^{-5}, and 1.32×10^{-5} m s^{-1} at V=1 cm s^{-1}, respectively. Hence, the corresponding Biot numbers for floc/granules from R1–R3 were 27.7, 53.0, and 77.1 at V=1 cm s^{-1}. Restated, in the investigated tests with aeration rate of 1–3 l min^{-1}, the Biot numbers for the present flocs/granules exceeded 100, yielding negligible external mass transfer resistance compared with internal diffusional resistance.

The floc pellets in R1 revealed minimal filament development at lower aeration rates but at a COD removal rate comparable to R2. Hence, DO deficiency was unlikely to have caused filament overgrowth in R2. However, after day 30, the COD removal rate was 75–81% for R1 and 86–96% for R2 and R3. The nutrient deficiency may be correlating with the growth of filaments in R2.

Nutrient deficiency, if occurring in R2 granules, should happen as well in R3 granules, as the external mass transfer presented no barrier to nutrient transport. However, the extended granular filaments were easily broken down under high shear, which apparently limited R3 filament growth. van Loosdrecht et al. (1995) and Kwok et al. (1998) reported that balance between biomass growth and detachment is necessary for biofilm stability. The surface erosion of extended filaments restricted their subsequent growth on the R3 granules. The lower shear rate in R2 preserved most extended filaments, eventually leading to system failure.

Distribution of EPS and stable granule structure

Microorganisms in high shear environments adhere by secreting EPS to resist damage of suspended cells by environmental forces (Trinet et al. 1991). The EPS constituents identified in this study included proteins, polysaccharides, humic acids, and lipids (Table 1 and Fig. 3). Wang et al. (2005) reported that the outer edge of aerobic granules consisted of poorly soluble EPS. McSwain et al. (2005) noted excess proteins in the core of granules. In this study, PN/PS ratios were 0.85–1.4 in R1 sludge pellets. Conversely, the PN/PS ratios for R2 and R3 granules were 3.4–5.3 and 3.4–6.2, respectively. McSwain et al. (2005) also reported high protein content in peptone and glucose-fed aerobic granules with a PN/PS ratio of 6.6–10.9. Tay et al. (2001) reported that hydrodynamic shear increased intracellular polysaccharide production. Di Iaconi et al. (2006) noted that hydrodynamic shear compacted the granules but cannot affect EPS content and compositions. The present study demonstrated that proteins, rather than polysaccharides, were enriched in the sheared granules, which is consistent with the results of McSwain et al. (2005). Chen et al. (2007) noted that proteins and dead cells were mainly distributed at the core regime of granules, while live cells and α-polysaccharides were located at the outer rim regime of the granules. Meanwhile, β-polysaccharides were distributed at the core and at the outer rim regimes of the phenol-fed granule. As Fig. 4 shows, the protein core apparently stabilizes granule integrity, but the possible role of β-polysaccharides on granule stability cannot be excluded, as it presents a network over the entire granule.

Granules under high shear exhibited redundant EPS (Fig. 3). However, the experimental results indicated filament overgrowth did not yield excess quantities of EPS. Quantities of extracted EPS have no correlation with filament overgrowth.

Conclusions

This study elucidated the effect of air aeration intensities on granule formation and EPS content in three identical sequential batch reactors (R1–R3). At a low aeration rate of 1 l min^{-1} (R1), sludge flocs were structurally compacted but failed to form large granules. Extracted EPS included 50.2–76.7 mg g^{-1} of proteins, 50.2–77.3 mg g^{-1} carbohydrates, and 74 mg g^{-1} humic substances. At a higher aeration rate of 3 l min^{-1} (R3), 1.0–1.5 mm granules with smooth outer surface were formed. The corresponding quantities of EPS were 309–537 mg g^{-1} of proteins, 61–109 mg g^{-1} carbohydrates, 49–92 mg g^{-1} humic substances, and 49–68 mg g^{-1} lipids. At an intermediate aeration rate of 2 l min^{-1} (R2), 3.0–3.5 mm granules formed with filaments covering the outer surface of the granules. The corresponding quantities of EPS extracted from R2 were 256–498 mg g^{-1} of proteins, 55.5–104 mg g^{-1} carbohydrates, 56–93 mg g^{-1} humic substances, and 50–70 mg g^{-1} lipids. Reactor R2 eventually failed with overgrowth of filaments. The EEM spectra clearly revealed proteins and humic substances in the sludge and granule samples. Multiple staining and imaging by CLSM revealed proliferating filaments with active biomass (proteins and β-polysaccharides) at the surface of R2 granules. The R3 granules exhibited a compact interior structure with a non-cellular core composed mainly of proteins and β-polysaccharides.

Intermediate to high hydrodynamic shear accelerates granule formation and overproduction of proteins in the granule core. Filament overgrowth was noted only at an intermediate aeration rate, probably due to nutrient deficiency in the liquid phase. High aeration shear eroded filaments at the granule surface and limited their subsequent growth. However, EPS composition revealed no correlation with proliferation of filamentous microorganisms. This study showed that aeration intensity could be used to manipulate granule stability, thereby affecting reactor performance in applications.

References

Adav SS, Chen MY, Lee DJ, Ren NQ (2007) Degradation of phenol by aerobic granules and isolated yeast Candida tropocalis. Biotechnol Bioeng 96:844–852

APHA (1998) Standard methods for the examination of water and wastewater, 20nd edn. American Public Health Association, Washington, DC

Arrojo B, Mosquera-Corral A, Garrido JM, Mendez R (2004) Aerobic granulation with industrial wastewater in sequencing batch reactors. Water Res 38:3389–3399

Beun JJ, Hendriks A, van Loosdrecht MCM, Morgenroth E, Wilderer PA, Heijnen JJ (1999) Aerobic granulation in a sequencing batch reactor. Water Res 33:2283–2290

Chen W, Westerhoff P, Leenheer JA, Booksh K (2003) Fluorescence excitation-Emission matrix regional integration to quantify spectra for dissolved organic matter. Environ Sci Technol 37:5701–5710

Chen MY, Lee DJ, Tay JH (2007) Distribution of extracellular polymeric substances in aerobic granules. Appl Microb Biotechnol 73:1463–1469

Di Iaconi C, Ramadori R, Lopez A, Passino R (2006) Influence of hydrodynamic shear forces on properties of granular biomass in a sequencing batch biofilter reactor. Biochem Eng J 30:152–157

Frolund B, Griebe T, Nielsen PH (1995) Enzymatic activity in the activated-sludge floc matrix. Appl Microbiol Biotechnol 43:755–761

Gaudy AF (1962) Colorimetric determination of protein and carbohydrate. Ind Water Wastes 7:17–22

Gaval G, Pernell JJ (2003) Impact of the repetition of oxygen deficiencies on the filamentous bacteria proliferation in activated sludge. Water Res 37:1991–2000

Hu L, Wang J, Wen X, Qian Y (2005) The formation and characteristics of aerobic granules in sequencing batch reactor (SBR) by seeding anaerobic granules. Process Biochem 40:5–11

Hwang KJ, You SF, Don TM (2006) Disruption kinetics of bacterial cells during purification of poly-beta-hydroxyalkanoate using ultrasonication. J Chin Inst Chem Eng 37:209–216

Kim SH, Choi HC, Kim IS (2004) Enhanced aerobic floc-like granulation and nitrogen removal in a sequencing batch reactor by selection of settling velocity. Water Sci Technol 50:157–162

Kwok WK, Picioreanu C, Ong SL, van Loosdrecht MCM, Ng WJ, Heijnen JJ (1998) Influence of biomass production and detachment forces on biofilm structures in a biofilm airlift suspension reactor. Biotechnol Bioeng 58:400–407

Li ZH, Kuba T, Kusuda T (2006) Selective force and mature phase affect the stability of aerobic granule: An experimental study by applying different removal methods of sludge. Enzyme Microb Technol 39:976–981

Liu H, Fang HHP (2002) Extraction of extracellular polymeric substances (EPS) of sludges. J Biotechnol 95:249–256

Liu Y, Liu QS (2006) Causes and control of filamentous growth in aerobic granular sludge sequencing batch reactors. Biotechnol Adv 24:115–127

Liu Y, Tay JH (2002) The essential role of hydrodynamic shear force in the formation of biofilm and granular sludge. Water Res 36:1653–1665

Liu Y, Tay JH (2004) State of the art of biogranulation technology for wastewater treatment. Biotechnol Adv 22:533–563

Lopes FA, Vieira MJ, Melo LF (2000) Chemical composition and activity of a biofilm during the start-up of an airlift reactor. Water Sci Technol 41:105–111

Martins AMP, Heijnen JJ, Van Loosdrecht MCM (2003) Effect of dissolved oxygen concentration on sludge settleability. Appl Microbiol Biotechnol 62:586–593

McSwain BS, Irvine RL, Wilderer PA (2004) The influence of settling time on the formation of aerobic granules. Water Sci Technol 50:195–202

McSwain BS, Irvine RL, Hausner M, Wilderer PA (2005) Composition and distribution of extracellular polymeric substances in aerobic flocs and granular sludge. Appl Environ Microb 71:1051–1057

Morgan JW, Forster CF, Evison LM (1990) A comparative study of the nature of biopolymers extracted from anaerobic and activated sludges. Water Res 6:743–750

Morgenroth E, Sherden T, van Loosdrecht MCM, Heijnen JJ, Wilderer PA (1997) Aerobic granular sludge in a sequencing batch reactor. Water Res 31:3191–3194

Moy BYP, Tay JH, Toh SK, Liu Y, Tay STL (2002) High organic loading influences the physical characteristics of aerobic granules. Lett Appl Microbiol 34:407–412

Quarmby J, Forster CF (1995) An examination of the structure of UASB granules. Water Res 29:2449–2454

Rossetti S, Tomei MC, Nielsen PH, Tandoi V (2005) Microthrix parvicella, lamentous bacterium causing bulking and foaming in activated sludge systems: a review of current knowledge. FEMS Microbiol Rev 29:49–64

Sheng GP, Yu HQ (2006) Characterization of extracellular polymeric substances of aerobic sludge using three-dimensional excitation and emission matrix fluorescence spectroscopy. Water Res 40:1233–1239

Tay JH, Liu QS, Liu Y (2001) The effects of shear force on the formation, structure and metabolism of aerobic granules. Appl Microbiol Biotechnol 57:227–233

Tay JH, Liu QS, Liu Y (2004) The effect of upflow air velocity on the structure of aerobic granules cultivated in a sequencing batch reactor. Water Sci Technol 49:35–40

Trinet F, Heim R, Amar D, Chang HT, Rittmann BE (1991) Study of biofilm and fluidization of bioparticles in a three-phase fluidized-bed reactor. Water Sci Technol 23:1347–1354

van Loosdrecht MCM, Eikelboom D, Gjaltema A, Mulder A, Tijhuis L, Heijnen JJ (1995) Biofilm structures. Water Sci Technol 32:35–43

Wang Q, Du G, Chen J (2004) Aerobic granular sludge cultivated under the selective pressure as a driving force. Process Biochem 39:557–563

Wang ZW, Li, u Y, Tay JH (2005) Distribution of EPS and cell surface hydrophobicity in aerobic granules. Appl Microb Biotech 69:469–473

Wu ST, Huang CC, Yu ST, Too JR (2006) Effects of nitrogen and phosphorus on poly-beta-hydroxyalkanoate production by Ralstonia eutropha. J Chin Inst Chem Eng 37:501–508